

Bladder Paraganglioma: Clinicopathology and Magnetic Resonance Imaging Study of Five Patients

Jiuping Liang,¹ Hengguo Li,^{1*} Likun Gao,² Liang Yin,³ Lei Yin,⁴ Jiawen Zhang⁵

Purpose: To investigate the clinicopathology and magnetic resonance imaging (MRI) features of bladder paraganglioma, an extremely rare clinical entity.

Materials and Methods: Five patients with bladder paraganglioma (3 males and 2 females, 27-52 years old) were retrospectively reviewed. All cases underwent baseline MRI and contrast-enhanced scans, and three cases underwent diffusion weighted imaging (DWI) and cystoscopy. Cases were immunohistochemically examined with neuroendocrine markers (chromogranin and synaptophysin) and Ki-67, and histology was reviewed by a pathologist.

Results: Three cases exhibited painless gross hematuria, including one case with hypertension, whereas two cases were asymptomatic. One of the three patients who underwent cystoscopy was negative. The tumors were round (n = 1) or oval (n = 4) and located in the anterior wall (n = 1), posterior wall (n = 1), lateral wall (n = 2) or trigone (n = 1). All tumors were located in the submucosal or lamina propria. Four cases presented with well-circumscribed margins, whereas one case was poorly circumscribed. All tumors exhibited slight hyperintensity on T1-weighted images (T1WI) and hyperintensity with “salt and pepper” appearance on T2-weighted images (T2WI). DWI indicated strong hyperintensity, and all cases exhibited conspicuous enhancement after intravenous gadobenate dimeglumine (Gd-DTPA) injection. Pathological evaluation confirmed paraganglioma.

Conclusion: MRI plays an important role in the preoperative diagnosis of bladder paraganglioma. This rare condition has a characteristic round or oval appearance, located in the submucosal area, with slight hyperintensity on T1WI and hyperintensity with “salt and pepper” appearance on T2WI. DWI indicated strong hyperintensity and conspicuous enhancement on contrast-enhanced scans.

Keywords: paraganglioma; diagnosis; urinary bladder neoplasms; humans; tomography X-ray computed; magnetic resonance imaging; differential.

INTRODUCTION

Bladder paraganglioma is extremely rare and accounts for 0.06% of all bladder tumors and 1% of extra-adrenal pheochromocytomas.^(1,2-6) Pheochromocytomas are secreting catecholamine tumors, which originate in the chromaffin cells of the sympathetic nervous system; tumors that originate from extra-adrenal sites are referred to as paraganglioma.^(1,2,7-10) The most common symptoms are intermittent painless gross hematuria, paroxysmal hypertension, and micturitional attacks.^(2,3,11,12) However, approximately 17% patients are hormonally inactive,⁽¹³⁾ which makes it notoriously difficult to confirm an actual preoperative diagnosis.⁽¹⁴⁾ Cystoscopy and biopsy may provoke a hypertensive crisis and are therefore not recommended.^(5,14) Furthermore, the biological behavior of bladder paraganglioma is uncertain, and the histological features are not reliable to distinguish malignant from benign tumors.^(3,8,9,11,15,16)

Previous studies⁽¹¹⁾ suggest that tumor stage and complete resection are the most important prognostic variables in patients with bladder paraganglioma. Thus, preoperative imaging plays a crucial role, and magnetic resonance imaging (MRI) has the lowest false negative localization rate for the diagnosis of paraganglioma.⁽¹⁷⁾ The rare prevalence of this disorder renders it substantially more difficult to complete a comprehensive study. Therefore, this study summarizes the clinicopathology and MRI characteristics of bladder paraganglioma in a series of case reports. To the best of our knowledge, this is the first study to report the clinicopathology and MRI features of bladder paraganglioma.

MATERIALS AND METHODS

Study Patients

This retrospective study was approved by our local ethics committee, and all patients provided written in-

¹ Medical Imaging Center, The First Affiliated Hospital, Jinan University, Guangzhou 510630, China.

² Department of Pathology, Renmin Hospital of Wuhan University, Wuhan, 430060, China.

³ Department of Radiology, Shenzhen Baoan Hospital, Southern Medical University, Shenzhen 518101, China.

⁴ Department of Radiology, Provincial Clinical College, Fujian Medical University, Fuzhou 350001, China.

⁵ Medical Imaging Center, Nan Fang Hospital, Southern Medical University, Guangzhou 510515, China.

*Correspondence: Medical Imaging Center, The First Affiliated Hospital, Jinan University, Guangzhou 510630, China.

Tel: +86 20 38688583. E-mail: lhginu@263.net.

Received August 2015 & Accepted March 2016

Table 1. Clinical features of bladder paraganglioma.

Case	Sex	Age (years)	Size (mm)	Blood Pressure (mmHg)	Clinical Symptoms	Cystoscopy Findings	Preoperative Diagnosis
1	Male	52	60	152/87	Intermittent painless gross hematuria, urinary frequency, urgency	Not performed	Carcinoma
2	Male	37	35	118/70	Intermittent urinary pain, painless gross hematuria	Neoplasm	Carcinoma
3	Female	50	15	127/84	Painless gross hematuria	Neoplasm	Carcinoma
4	Female	33	40	114/82	Asymptomatic	Not performed	Leiomyoma
5	Male	27	35	118/80	Asymptomatic	No neoplasm	Isolated fibroma

formed consent. Five cases of bladder paraganglioma were enrolled at four hospitals from November 2011 to April 2014. The participants comprised 3 males and 2 females, with an age range of 27-52 years. The mean age of the participants was 39.80 ± 10.85 years.

MRI Examination

MRI examinations were performed with a Philips Achieva 1.5T (Philips, Amsterdam, The Netherlands), GE Signa HDxt 1.5T and a 3.0T magnetic resonance scanner (Signa Excite, General Electric, Fairfield, CT, USA), and Siemens Verio 3.0T (Siemens, Munich, Germany) MR scanners. The patients were placed in a supine position. A surface phased-array coil was used, and scanning was conducted with the following parameters.

Philips Achieva 1.5T: field of view (FOV), 370-82.8 mm; Mmatrix, 320×256 ; thickness, 5.5-6.6 mm; intersection gap, 0.725 mm; T1-weighted images (T1WI;

Echo Time [TE], 19.995; Repetition Time [TR], 500); T2-weighted images (T2WI; TE, 100; TR, 3624); fat saturated; and diffusion weighted imaging (DWI; TE, 67.448; TR, 1130.7) with b values of 0 and 800 s/mm^2 . GE Signa 1.5T: FOV, 310-420 mm; Mmatrix, 384×245 ; thickness, 4-7 mm; intersection gap, 1 mm; T1WI (TE, 1.7-7.7; TR, 3.4-480); T2WI (TE, 109-130; TR, 3200-3900); fat saturated; and DWI (TE, 89.2-9; TR, 2950-3650) with b values of 0 and 800 s/mm^2 .

GE Signa 3.0T: FOV, 340-400 mm; Mmatrix, 384×224 ; thickness, 4-5 mm; intersection gap, 1 mm; T1WI (TE, 1.8-7.5; TR, 180-500); T2WI (TE, 135.2; TR, 4000-4140); and fat saturated.

Siemens Verio 3.0T: FOV, 228-370 mm; Mmatrix, 320×320 ; thickness, 4-6 mm; intersection gap, 1 mm; T1WI (TE, 11; TR, 721-826); T2WI (TE, 70-98; TR, 4000-5190); and fat saturated.

Gadobenate dimeglumine (0.1 mmol/kg; Bayer Schering Pharma AG, Berlin-Wedding, Germany and CON-SUN, Guangzhou, China) was intravenously injected via a rapid bolus injection at a rate of 2-3 mL/s with a power injector (Spectris Solaris MR Injector System, Medrad, Incorporated, Pittsburgh, PA, USA). All MRI findings were independently analyzed by two radiologists (with 13 and 17 years of experience, respectively).

Pathological Examination

All specimens were investigated morphologically and immunohistochemically. All histological slides were retrospectively reviewed by a pathologist (with 8 years of experience) who was unaware of the MRI findings. The patient follow-up data were acquired from case histories. Formalin-fixed and paraffin-embedded specimens were cut into conventional 5- μm -thick sections, immunohistochemically stained, and examined. Immunohistochemical analysis was performed using an avidin-biotin-peroxidase complex (ABC) method.

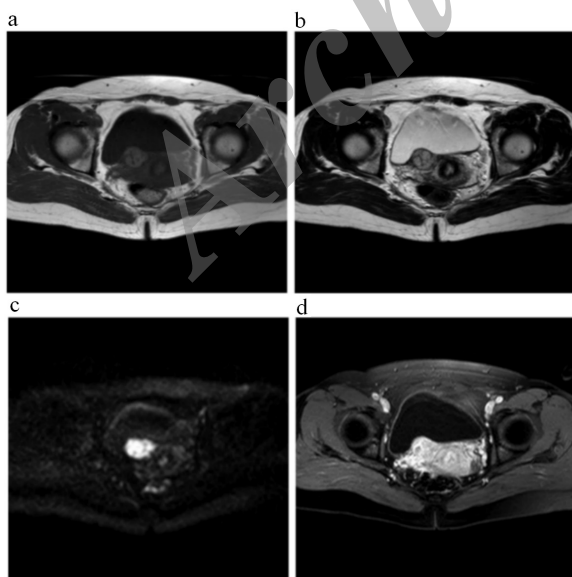


Figure 1. The tumors were round or oval appearance, located in the sub-mucosal area, with slight hyperintensity on T1WI (a) and hyperintensity with "salt and pepper" appearance on T2WI (b). Diffusion weighted imaging indicated strong hyperintensity (c) and conspicuous enhancement on contrast-enhanced scans (d).

Table 2. Pathology of bladder paraganglioma.

Case	Location	Morphology	Immunohistochemistry						
			Ki-67	S-100	Syn	CD56	p53	CgA	Vimentin
1	Submucosa	Tumor cells grew in “Zellballen pattern” separated by elaborate vascular septa; increased number of mitotic figures and focal necrosis.	50% +	+	-	+	+ (weakly)	-	
2	Submucosal and muscularis propria	Tumor cells characterized by round cells arranged in “Zellballen pattern” separated by fine vascular network; tumor cells contained abundant cytoplasm with an eosinophilic granular appearance; mitotic figures occasionally identified.	3% +	+	+			+	+/-
3	Muscularis propria	Tumor cells grew in “Zellballen pattern” embedded in a fibrous vascularized network; round cells contained abundant cytoplasm with an eosinophilic granular appearance; mitotic figures were not common.	3% +	+	+++	+++		+++	
4	Submucosa	Tumor cells grew in “Zellballen pattern” embedded in a fibrous vascular network; cells exhibited mild atypia.	2% +	+	+++		+ (weakly)	+++	
5	Submucosal and muscularis propria	Tumor cells grew in “Zellballen pattern” separated by elaborate vascular septa; tumor cells had abundant cytoplasm with an eosinophilic granular appearance; nuclei exhibited mild atypia; mitotic figures were inconspicuous; tumor capsule was incomplete; lymphatic invasion was identified.	5% +	+	+		+	+	

Abbreviations: Syn, synaptophysin; CgA, chromogranin; S-100, sustentacular cell.

RESULTS

Clinical Features

Three cases comprised painless gross hematuria (1 case with hypertension), whereas two cases were asymptomatic with an increased blood pressure (BP) of 200-240 mmHg (systolic BP: case 4, 240 mmHg; case 5, 200 mmHg) at the beginning of the resection. Three cases underwent cystoscopy, in which 2 cases exhibited neoplasm and 1 case was negative. All cases underwent surgery. The detailed clinical profiles of the patients are summarized in **Table 1**.

MRI Features

The tumors were round (n = 1) or oval (n = 4) and located in the anterior wall (n = 1), lateral wall (n = 2), posterior wall (n = 1), or trigone (n = 1). All tumors were located in the submucosa. All tumors demonstrated slight hyperintensity on the T1WI (**Figure 1a**). Furthermore, the tumors demonstrated hyperintensity and a “salt and pepper” appearance on the T2WI (**Figure**

1b). DWI was conducted in three patients, which indicated strong hyperintensity (**Figure 1c**). All tumors demonstrated conspicuous enhancement on the contrast-enhanced images (**Figure 1d**). Four tumors exhibited well-circumscribed margins, while one tumor (case 1) was poorly circumscribed and had invaded the pelvic wall. No lymph nodes or distant metastases were identified in any of the cases.

Pathology

All tumors were round or oval, and all cases were located in the submucosa or lamina propria. The tumor cells were arranged in a “Zellballen” pattern, round and acidophilic, and embedded in a fibrous septa, which was richly vascularized (**Figure 2a**). Nuclear pleomorphism and mitotic figures were occasionally identified. Immunohistochemically, these cells were positive for vimentin, p53, and neuroendocrine markers, such as synaptophysin (Syn), chromogranin (CgA) (**Figure 2b**), and neuronal cell adhesion molecules 56 (CD 56).

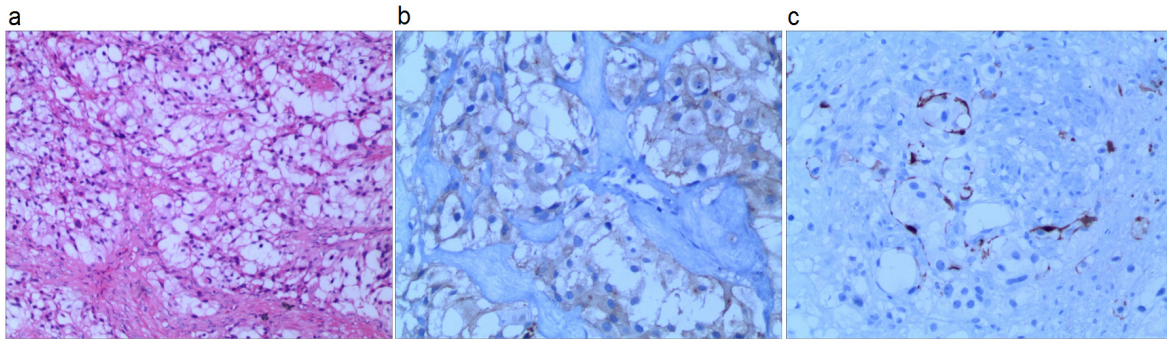


Figure 2. The tumor comprised large polygonal cells with clear cytoplasm in a typical “Zellballen growth” pattern with elaborate vascular septa (a). Immunostaining for the neuroendocrine marker chromogranin A was positive (b). Sustentacular cells were highlighted on immunostaining for S-100 protein (c).

Sustentacular cells were immunostained for S-100 protein (Figure 2c). The Ki-67 indices were low (< 5%) with the exception of one case. The detailed pathology features are summarized in Table 2.

DISCUSSION

The diagnosis of bladder paraganglioma is often confirmed by increased levels of catecholamines and their urinary and serum metabolites.^(12,18,19) Biochemical investigations were not performed on all cases in this series of patients because bladder paraganglioma was not considered preoperatively given the lack of classical signs and symptoms. Cystoscopy and biopsy were avoided, which may provoke a hypertensive crisis following insufficient preparation.^(5,14) In this study, two cases exhibited a sudden hypertensive crisis at the beginning of resection, which was controlled by medical intervention. One of the three cases who underwent cystoscopy was negative as a result of the submucosal tumor location and the cover provided by an intact epithelium. Therefore, a preoperative ultrasound, CT scan, and MRI were important for a definitive therapy.⁽⁵⁾ MRI is superior to CT scan in diagnostic sensitivity and specificity for the submucosal origin of the tumor because of its inherent tissue contrast resolution and multiple parametric imaging.^(2,9,10,12) However, reports regarding MRI features of bladder pheochromocytoma are rare, and previous publications involve single or very small case reports.^(2,4,9,12,20,21)

Bladder paraganglioma originates in the paraganglionic cells that migrate into the bladder wall.^(3,13,22) Li and colleagues⁽²³⁾ reported that approximately 40% of bladder paraganglioma tumors were located in the submucosa, which may represent a key ultrasound imaging characteristic of bladder paraganglioma. However, Cheng and colleagues⁽¹¹⁾ reported that approximately 94% of tumors involved the lamina propria of the bladder wall. In

this study, MRI indicated the location of all the masses was the submucosal layer, which is consistent with previous studies.^(6,8,13,14,19,20,23,24) Furthermore, the pathology results also demonstrated that all masses were located in the submucosal or lamina propria. Nevertheless, the anatomical site predilection has been controversial in previous reports.^(3,11,23) There was no site predilection identified in this study, which is in accordance with a previous study.⁽²⁵⁾ In this study, all masses exhibited slight hyperintensity on the T1WI and fat saturation, which is consistent with previous research.⁽¹²⁾ Wang and colleagues⁽²¹⁾ suggested that lesions that exhibit homogeneous hyperintensity on T1WI are the key MRI features of bladder paraganglioma; however, the reason for the slight hyperintensity on T1WI remains unknown. Electron microscopic studies have indicated the presence of dark brown intracytoplasmic granules^(3,7,8,15) and melanin pigments⁽²⁶⁾ in tumor cells, which may explain the increased signal intensity on T1WI; however, these findings require further confirmation. While all tumors exhibited hyperintensity on T2WI and fat saturation, the “salt and pepper” appearance may be an important MRI feature, which is consistent with the pathology results and the MR features of carotid body tumor and glomus jugular tumor.⁽²⁷⁾ In this study, all tumors exhibited conspicuous enhancement because of their vascularity, which is in accordance with previous studies.^(14,21,23) Furthermore, this enhancement is an important diagnostic feature that differentiates bladder paraganglioma from other bladder tumors.⁽²⁴⁾ Wang and colleagues⁽²¹⁾ reported that the mean ADC values of bladder paraganglioma were lower than the values for bladder cancer. In this study, DWI was conducted in three patients and indicated strong hyperintensity, which may represent another MR imaging characteristic of bladder paraganglioma.

It is very difficult to obtain an actual preoperative diag-

nosis in asymptomatic bladder paragangliomas. Histological features and immunohistochemistry have been important for the differential diagnosis of other bladder tumors;^(1,25) in some cases, these approaches are the only alternative. In this study, the tumor cells were round or polygonal epithelioid and arranged in a pattern of classic Zellballen with elaborate vascular septa. However, this feature is not always conspicuous, and some tumors grow diffusely. Individual tumor cells are most often polygonal with a moderate amount of granular, eosinophilic to amphophilic cytoplasm. Some cells may morphologically mimic neuronal or ganglion cells. Nuclear hyperchromasia and pleomorphism may be prominent features; however, these features are not reliable predictors of malignant behavior. These cells were characteristic of positive immunostaining for neuroendocrine markers, such as Syn, CgA, and CD56. Positive nuclear staining for S-100 protein highlighted the sustentacular cells. In addition, two cases expressed the limited positivity of p53. The role of p53 in pheochromocytoma tumorigenesis is unclear. Petri and colleagues⁽²⁸⁾ have reported that although there is frequent loss of the p53 locus on 17p, the p53 gene does not appear to play a major role in pheochromocytoma tumorigenesis. The antibody p53 (Dako, DO-7) reacts with the wild type and mutant type of the p53 protein. Thus, we suggest that the limited positivity of p53 should be considered in wild type expression.

The paraganglioma biological behavior is uncertain, and previous reports^(3,8,9,11,15,16) have indicated that histological features were not reliable to distinguish malignant from benign tumors. The most recent World Health Organization classification of pheochromocytomas and paragangliomas defined malignancy as the presence of metastases, not local invasion.⁽²⁹⁾ In this study, the tumor capsule of case 5 was incomplete, and lymphatic invasion was identified, as local invasion is a poor predictor of aggressive behavior, and the absence of invasion does not obviate the development of metastasis.⁽³⁰⁾ Thus, while we cannot view case 5 as malignant, the patient should be followed over time.

Necrosis and an increased number of mitotic figures have previously been associated with a more aggressive prognosis in patients with paraganglioma.⁽³¹⁾ Case 1 exhibited malignant biological behavior that suggested tumor necrosis, an increased mitotic index, and a high (50%) Ki-67 index. This case required additional follow-up; however, no recurrence or metastases occurred in an 8 month follow-up period. Kang and colleagues⁽⁸⁾ reported that long term follow-up was required. Microscopic sections may demonstrate what appears to

be an invasion of lamina propria of the bladder wall; thus, the bladder paraganglioma may often be judged for malignant tumor prior to operation. The major differential diagnoses of bladder paraganglioma include the following: granulosa cell tumor, a nested variant of urothelial carcinoma, metastatic large-cell neuroendocrine carcinoma, and malignant melanoma.⁽¹¹⁾ Awareness of these rare diseases is essential to prevent misinterpretation. The lack of a “Zellballen growth” mode and fine vascular stroma, absence of a sustentacular staining pattern of S-100 protein, and negative immunostaining of neuroendocrine markers easily discriminate these tumors from bladder paraganglioma.⁽¹¹⁾ When some atypia and mitotic features are present, it is easy to understand how a misdiagnosis of conventional urothelial carcinoma may be made; however, specific immunohistochemical stains may be helpful. It should be pointed out that metastatic neuroendocrine tumors also express neuroendocrine markers; however, the histological characteristics, including necrosis, cellular anaplasia, and mitotic figures, and the absence of a sustentacular staining pattern of S-100 protein distinguish them from paraganglioma. Furthermore, in uncommon cases, bladder paraganglioma contains melanin pigment, similar to malignant melanoma.⁽²⁶⁾ Melanomas do not express neuroendocrine markers, which may differentiate each other. However, none of the current cases had melanin pigments. Furthermore, a rare composite paraganglioma-ganglioneuroma may occur in the urinary bladder;⁽³²⁾ this tumor may contain a substantial component of ganglioneuroma that consists of mature ganglion and spindle cells that merge with the classical paraganglioma component. To identify unique components, such as ganglioneuroma, neuroblastoma, or ganglioneuroblastoma, a malignant peripheral nerve sheath tumor (MPNST; malignant schwannoma) in the tumor may facilitate the correct diagnosis of composite paraganglioma/pheochromocytoma.

CONCLUSIONS

In conclusion, MRI plays an important role in the preoperative diagnosis of bladder paraganglioma, with a relatively characteristic MR appearance, including a round or oval shape and submucosal location. T1WI exhibited slight hyperintensity, whereas T2WI indicated hyperintensity with a “salt and pepper” appearance. DWI exhibited strong hyperintensity and conspicuous enhancement. Pathological evaluation suggested paraganglioma as the final diagnosis. However, several limitations must be considered in the interpretation of these clinical findings. First, because of the rare prevalence

of this disorder, this study comprised a small sample of patients. Furthermore, a retrospective design was used. Thus, a prospective and multicenter study is needed to elucidate the clinical findings revealed in these case reports. Nevertheless, the current case report provides novel insights regarding the rare clinical condition of bladder paraganglioma.

CONFLICTS OF INTEREST

None declared.

REFERENCES

1. Bohn OL, Pardo-Castillo E, Fuertes-Camilo M. Urinary bladder paraganglioma in childhood: a case report and review of the literature. *Pediatr Dev Pathol*. 2011;14:327-32.
2. Wong-You-Cheong JJ, Woodward PJ, Manning MA, Davis CJ. Neoplasms of the Urinary Bladder: Radiologic-Pathologic Correlation. *Radiographics*. 2006;26:1847-68.
3. Leestma JE, Price EBJ. Paraganglioma of the urinary bladder. *Cancer*. 1971;28:1063-73.
4. Ansari MS, Goel A, Goel S, Durairajan LN, Seth A. Malignant paraganglioma of the urinary bladder. A case report. *Int Urol Nephrol*. 2001;33:343-5.
5. Dahm P, Gschwend JE. Malignant Non-Urothelial Neoplasms of the Urinary Bladder: A Review. *Eur Urol*. 2003;44:672-81.
6. Liu Y, Dong SG, Dong Z, Mao X, Shi XY. Diagnosis and treatment of pheochromocytoma in urinary bladder. *J Zhejiang Univ Sci B*. 2007;8:435-8.
7. Lam KY, Loong F, Shek TW, Chu SM. Composite paraganglioma-ganglioneuroma of the urinary bladder: a clinicopathologic, immunohistochemical, and ultrastructural study of a case and review of the literature. *Endocrine Pathol*. 1998;9:363-73.
8. Kang WY, Chai CY, Shen JT. Paraganglioma of the urinary bladder: a case report. *The Kaohsiung J Med Sci*. 2003;19:136-40.
9. Halefoglu AM, Miroglu C, Uysal V, Mahmutoglu A. Malignant paraganglioma of the urinary bladder. *Eur J Radiol Extra*. 2006;58:53-8.
10. Tsai CC, Wu WJ, Chueh KS, et al. Paraganglioma of the urinary bladder first presented by bladder bloody tamponade: two case reports and review of the literatures. *Kaohsiung J Med Sci*. 2011;27:108-13.
11. Cheng L, Leibovich BC, Cheville JC, et al. Paraganglioma of the Urinary Bladder Can Biologic Potential Be Predicted? *Cancer*. 2000;88:844-52.
12. Celiktaş M1, Okur N, Aikimbaev KS, Binokay F, Sert M, Akgül E. Bladder pheochromocytoma encountered on sonography. *Australas Radiol*. 2004;48:398-400.
13. Das S, Bulusu NV, Lowe P. Primary vesical pheochromocytoma. *Urology*. 1983;21:20-5.
14. Xu DF, Chen M, Liu YS, Gao Y, Cui XG. Non-functional paraganglioma of the urinary bladder: a case report. *J Med Case Rep*. 2010;4:216.
15. Dewan M, Rasheed M, Elmalik EM, Ansari MA, Morad N. Lessons to be learned: a case study approach Paraganglioma of the urinary bladder. *J R Soc Promot Health*. 2001;121:193-8.
16. Huang KH, Chung SD, Chen SC, et al. Clinical and pathological data of 10 malignant pheochromocytomas: long-term follow up in a single institute. *Int J Urol*. 2007;14:181-5.
17. Erickson D, Kudva YC, Ebersold MJ, et al. Benign Paragangliomas: Clinical Presentation and Treatment Outcomes in 236 Patients. *J Clin Endocrinol Metab*. 2001;86:5210-6.
18. Whalen RK, Althausen AF, Daniels GH. Extra-adrenal pheochromocytoma. *J Urol*. 1992;147:1-10.
19. Al-Zahrani AA. Recurrent urinary bladder paraganglioma. *Adv Urol*. 2010:912125.
20. Usuda H, Emura I. Composite paraganglioma-ganglioneuroma of the urinary bladder. *Pathol Int*. 2005;55:596-601.
21. Wang H, Ye H, Guo A, et al. Bladder paraganglioma in adults: MR appearance in four patients. *Eur J Radiol*. 2011;80:e217-20.
22. Zimmerman IJ, Biron RE, Macmahon HE. Pheochromocytoma of the urinary bladder. *N Engl J Med*. 1953;249:25-6.
23. Li Y, Guo A, Tang J, et al. Evaluation of sonographic features for patients with urinary bladder paraganglioma: a comparison with patients with urothelial carcinoma. *Ultrasound Med Biol*. 2014;40:478-84.
24. Athyal RP, Al-Khawari H, Arun N, Abul F, Patrick J. Urinary bladder paraganglioma in a case of von Hippel-Lindau disease. *Australas Radiol*. 2007;51:B67-B70.
25. Menon S, Goyal P, Suryawanshi P, et al. Paraganglioma of the urinary bladder: a clinicopathologic spectrum of a series of 14 cases emphasizing diagnostic dilemmas. *Indian J Pathol Microbiol*. 2014;57:19-23.
26. Moran CA, Albores-Saavedra J, Wenig BM, Mena H. Pigmented extraadrenal paragangliomas: a clinicopathologic and immunohistochemical study of five cases. *Cancer*. 1997;79:398-402.
27. Lee KY, Oh YW, Noh HJ, et al. Extraadrenal paragangliomas of the body: imaging features. *AJR Am J Roentgenol*. 2006;187:492-504.
28. Petri BJ, Speel EJ, Korpershoek E, et al. Frequent loss of 17p, but no p53 mutations or protein overexpression in benign and malignant pheochromocytomas. *Mod Pathol*.

- 2008;21:407-13.
29. DeLellis, Ronald A., ed. Pathology and genetics of tumours of endocrine organs. Vol. 8. IARC, 2004.
 30. Tischler AS. Pheochromocytoma and extra-adrenal paraganglioma: updates. Arch Pathol Lab Med. 2008;132:1272-84.
 31. Lack EE, Cubilla AL, Woodruff JM. Paragangliomas of the head and neck region. A pathologic study of tumors from 71 patients. Hum Pathol. 1979;10:191-218.
 32. Chen CH, Boag AH, Beiko DT, Siemens DR, Froese A, Isotalo PA. Composite paraganglioma-ganglioneuroma of the urinary bladder: a rare neoplasm causing hemodynamic crisis at tumour resection. Can Urol Assoc J. 2009;3:E45-8.

Archive of SID